

A Reinvestigation of the Physical Properties of Pismis 3 based on 2MASS Photometry

Tadross A. L.

National Research Institute of Astronomy and Geophysics, 11421 - Helwan, Cairo, Egypt
altadross@nriag.sci.eg

Received 2007 May 31; accepted 2008 April 11

Abstract As a continuation of a series of work, we aim to refine and re-determine the physical parameters of previously rarely or un-studied open star clusters with good quality CMDs using Near-IR *JHK* photometry. Here we present a morphological analysis of the 2MASS database (the digital “Two Micron All Sky Survey”) for the open cluster Pismis 3. Some of the physical parameters are estimated for the first time, and some others, re-determined.

Key words: techniques: photometric — Galaxy: open clusters and associations — stars: luminosity function — stellar clusters: individual: Pismis 3

1 INTRODUCTION

A deep photometric and astrometric analysis in the open star cluster Pismis 3 can be carried out by using the 2MASS¹ database. The 2MASS surveys have proven to be a powerful tool in the analysis of the structure and stellar content of open clusters (cf. Bonatto & Bica 2003; Bica et al. 2003). It uniformly scans the entire sky in three near-IR bands, *J*(1.25 μm), *H*(1.65 μm) and *K_s*(2.17 μm), with two highly automated 1.3-m telescopes equipped with a three channel camera, each channel consisting of a 256 \times 256 array of HgCdTe detectors. The photometric uncertainty of the data is less than 0.155 mag with *K_s* \sim 16.5 mag photometric completeness. Further details can be found at the website of 2MASS.

Pismis 3 (C0829–3830, OCL 731) is situated in the southern Milky Way at 2000.0 coordinates $\alpha = 08^{\text{h}} 31^{\text{m}} 22^{\text{s}}$, $\delta = -38^{\circ} 39' 00''$; $\ell = 257.865^{\circ}$, $b = +0.502^{\circ}$. The name takes from the astronomer who in the late fifties (Pismis 1959) compiled a catalogue of 2 globular and 24 new open star clusters in the Galactic Plane between $\ell = 225^{\circ}$ and $\ell = 353^{\circ}$. Carraro & Ortolani (1994), hereafter CO94, obtained CCD *BV* photometry for Pismis 3 and its nearby field. Their analysis suggests that it is of intermediate age (about 2 Gyr) and is metal poor ($Z = 0.008$). They derived a color excess $E(B - V) = 1.35$, and an apparent distance modulus ($m - M$) = 14.70 mag (about 1.5 kpc distant from the Sun). In the present study, we estimated most of the fundamental parameters of Pismis 3, i.e., the age, reddening, distances (from the sun, the galactic plane and the galactic center), dimensions (cluster’s diameter, core radius and tidal radius), luminosity function, mass function, total mass, relaxation time, and mass segregation. The relevant examples are NGC 1883, NGC 2059, NGC 7086 (Tadross 2005), and NGC 7296 (Tadross 2006). Figure 1 shows the blue image of Pismis 3 as quoted from Digitized Sky Surveys (DSS)².

This paper is organized as follows: Section 2, data extraction; Section 3, cluster center and radii; Section 4, CMD analysis (membership richness - reddening - distances - age, and metallicity); Section 5, luminosity function; Section 6, mass functions and total mass; Section 7, mass segregation, dynamical state, and finally the results are summarized and listed in a table.

¹ <http://www.ipac.caltech.edu/2MASS>

² <http://cadwww.dao.nrc.ca/cadcbn/getdss>

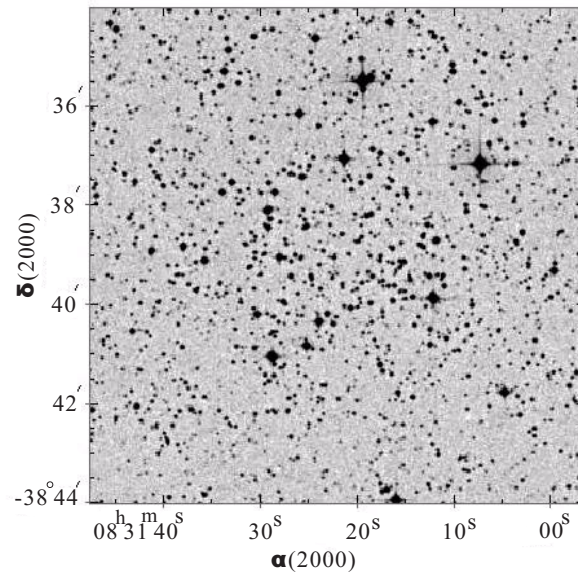


Fig. 1 Blue image of Pismis 3, taken from Digitized Sky Surveys (DSS). North is up, east on the left.

2 DATA EXTRACTION

Data extraction have been performed using the known tool of VizieR³. The number of stars in the region of Pismis 3 within a preliminary radius of 10 arcmin is found to be 4390. In order to maximize the statistical significance and representativeness of background star counts, an external area (the same size as the cluster) was used as a comparison field sample. This external sample lies at 1 degree away from the cluster's center.

Before counting the stars for estimating the cluster's properties with *JHK 2MASS* photometry, we applied a cutoff of photometric completeness ($J < 16.5$) to both the cluster and comparison field to avoid over-sampling, i.e., to avoid spatial variations in the number of faint stars which are numerous, affected by large errors, and may include spurious detection (Bonatto et al. 2004). Also, in this respect, for greater accuracy, we restricted to stars with observational uncertainties $\epsilon_{J, H, K} < 0.2$ mag.

3 THE CLUSTER CENTER AND RADII

The cluster center is defined as the location of maximum stellar density in the cluster area, and is found by fitting a Gaussian to the profile of star counts in right ascension (α) and declination (δ), see Tadross (2004, 2005, 2006). The estimated center is found to lie at $\alpha = 127.84089 \pm 0.003$ and $\delta = -38.64478 \pm 0.002$ degrees, which differ from WEBDA⁴ by 0.2 s in right ascension and 18.8 arcsec in declination.

To determine the cluster's minimum radius, core radius and tidal radius, the radial surface density of the stars $\rho(r)$ should be obtained first. The tidal radius determination is made possible by the spatial coverage and uniformity of *2MASS* photometry, which allows one to obtain reliable data on the projected distribution of stars over extended regions around clusters (Bonatto et al. 2005). We found that the background contribution level corresponds to the average number of stars included in the comparison field sample is ~ 18 stars per arcmin². Applying the empirical profile of King (1962), the cluster's minimum apparent radius turns out to be 3.5 arcmin, as shown in Figure 2. Knowing the cluster distance from the sun in parsecs (Sect. 4), the cluster and core radii are found to be 2.2 and 0.2 pc, respectively. Applying the equation of Jeffries et al. (2001), the tidal radius (R_t) of Pismis 3 is found to be ~ 12 pc. Consequently, the distances of the cluster from the galactic plane, Z , and its projected distances from the Sun, X_\odot , Y_\odot , are 18.0 pc,

³ <http://vizier.u-strasbg.fr/viz-bin/VizieR?-source=2MASS>

⁴ <http://obswww.unige.ch/webda/navigation.html>

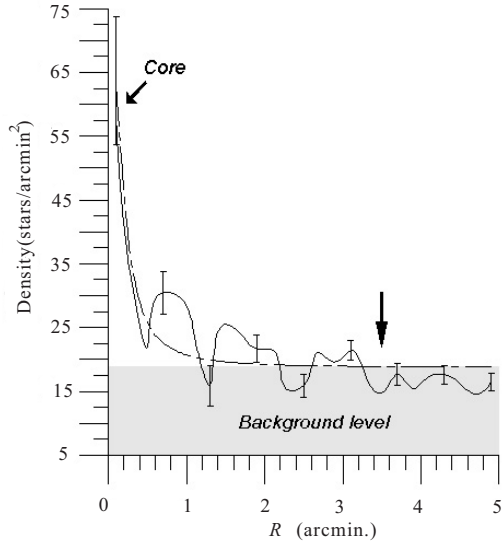


Fig. 2 Radial distribution of the surface density of Pismis 3 (solid curve). The vertical short bars represent Poisson errors, and the dashed line represents the fitting of King (1962). The upper arrow refers to the core region, and the lower, to the apparent minimum radius of the cluster. The shaded region shows the mean level of the comparison field density, taken to be ~ 18 stars per arcmin².

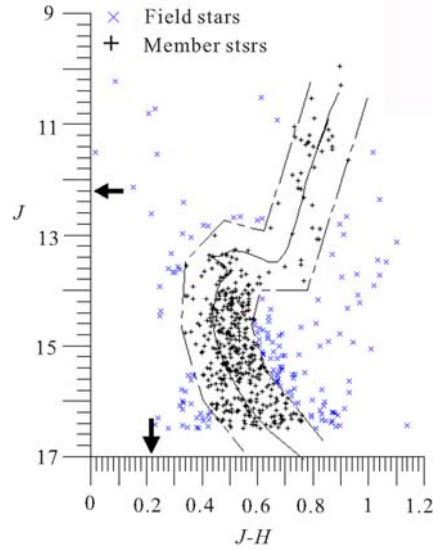


Fig. 3 Padova solar isochrone with log age = 9.35 (2.24 Gyr) is fitted to the $J \sim (J - H)$ CMD of Pismis 3. Dashed curves represent the color and magnitude filters used in reducing the field contamination of the cluster. The horizontal and vertical arrows refer to the values of distance modulus and color excess on the vertical and horizontal axes, respectively.

-2.0 , and 0.44 kpc, respectively. The distance from the galactic center, R_g , is 8.7 or 8.0 kpc, according as the galactocentric distance of the sun R_o is taken to be 8.0 or 7.2 kpc, according to Reid (1993) or Bica et al. (2006). It is found that R_g agrees with, but Z is larger than the values obtained by Salaris et al. (2004).

4 COLOR-MAGNITUDE DIAGRAM ANALYSIS

Because of the low galactic latitude of Pismis 3, the background field of the cluster is crowded (≈ 18 stars per arcmin²), and the observed CMD is contaminated. Figure 3 shows the CMD of Pismis 3, with the magnitude completeness limit and the color filter for the stars within the apparent cluster radius, indicated. In total 450 stars have been classified as cluster members. The membership criterion adopted here for inclusion of stars in the CMD is that they must be close to the cluster main sequence, deviating by not more than about 0.15 mag (the accepted stars are those marked with plus signs between the two dashed curves in Fig. 3). On this basis, the fundamental photometrical parameters of the cluster (reddening, distance modulus, age and metal content) can be determined simultaneously, by fitting a Padova isochrone to the CMD.

Several fittings were applied to the $J \sim (J - H)$ of Pismis 3 using the Bonatto et al. (2004) isochrones of solar metallicity with different ages. $R_V = 3.2$, $A_J = 0.276 \times A_V$, and $E(J - H) = 0.33 \times E(B - V)$ were used for the reddening and absorption transformations, according to Dutra, Santiago & Bica (2002) and the references therein. The overall shape of the CMD is found to be well reproduced with isochrones of age 2.24 Gyr. The apparent distance modulus is 12.20 ± 0.10 mag, accordingly the intrinsic distance modulus is $(m - M)_o$ is 11.60 ± 0.10 mag, corresponding to a distance of 2090 ± 95 pc. On the other hand, the color excess $E(J - H)$ is 0.22 mag, which corresponds to $E(B - V) = 0.67$ mag. It is found that $[\text{Fe}/\text{H}]$ is in agreement with, but the age is smaller than the values obtained by Salaris et al. (2004). It is worth

mentioning that the noticed differences of the main parameters for Pismis 3 between the present work and CO94 is mainly due to the difference of the metal content of the used isochrone.

5 LUMINOSITY FUNCTION

The observed stars were counted in the absolute magnitude M_J after applying the distance modulus derived above. Cutoffs in the color and magnitude filters were applied to the cluster and comparison field stars. The magnitude bin intervals are taken to be $\Delta M_J = 0.50$ mag. Figure 4 displays the difference in the number of stars in a given magnitude bin between the stars in the cluster (dashed area) and in the comparison field (white area). The dotted area represents the background subtracted LF . The scale of the observed J magnitude appears along the upper axis. From the LF of Pismis 3 we infer that the more massive stars are more centrally concentrated while the peak value lies at the fainter magnitude bin (Montgomery et al. 1993) corresponding to $J \approx 15.3$ mag, i.e. $M_J \approx 3.7$ mag.

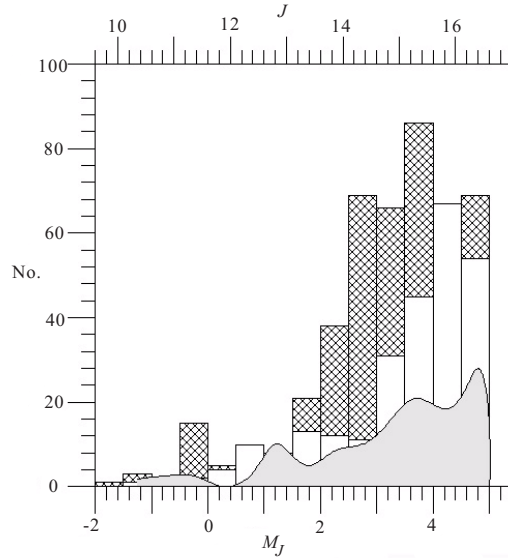


Fig. 4 Spatial distribution of luminosity function for Pismis 3 in terms of the absolute magnitude M_J . The color and magnitude filter cutoffs have been applied to the cluster (dashed area) and the comparison field (white area). The dark curved area represents the background subtracted LF . The scale of observed J magnitude appears along the upper axis.

6 MASS FUNCTION AND TOTAL MASS

Given the luminosity function, the mass function and then the total mass of the cluster can be derived. To obtain MF from LF , the theoretical evolutionary track of Bonatto et al. (2004) with solar metal abundance ($Z = 0.019$) and age of 2.24 Gyr is used. Here, a polynomial equation of fourth degrees was used for the cluster members in the range $-1.75 \leq M_J \leq 4.75$:

$$M/M_{\odot} = 3.13 - 0.66 M_J - 0.10 M_J^2 + 0.051 M_J^3 - 0.005 M_J^4.$$

A step-plot was constructed for the cluster stellar masses showing the number of stars at 0.5 intervals between $0.65 \sim 3.65 M_{\odot}$, see Figure 5. Using a least-square fit, the slope of IMF is found to be $\Gamma = -2.37 \pm 0.25$, which is in rough agreement with Salpeter (1955). In this respect, the total mass of the cluster was estimated by summing up the stars in each bin weighted by the mean mass of that bin. It yielded a minimum cluster mass of $\sim 560 M_{\odot}$.

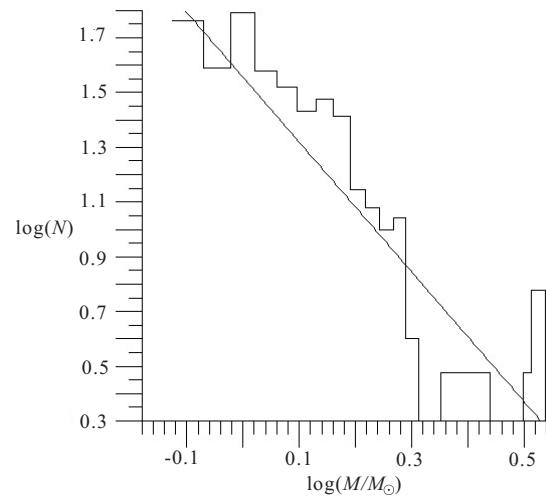


Fig. 5 Mass function of Pismis 3. The slope of the initial mass function IMF is $\Gamma = -2.37 \pm 0.25$. Correlation coefficient is 0.90.

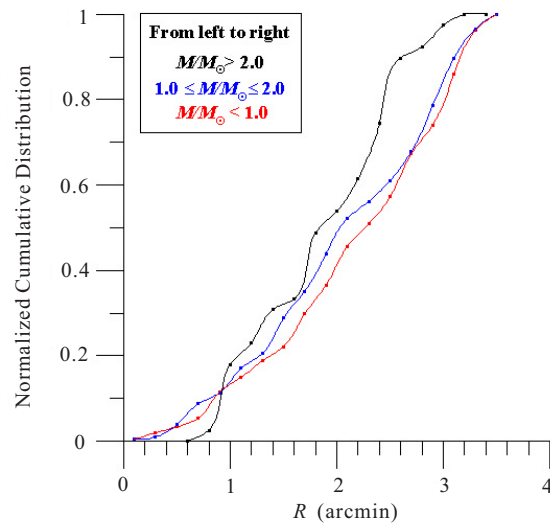


Fig. 6 Mass segregation in Pismis 3. From left to right, the curves represent the mass ranges $\mathcal{M}/\mathcal{M}_{\odot} > 2.0$, ($M_J: -0.1 \sim 1.5$); $1.0 \leq \mathcal{M}/\mathcal{M}_{\odot} \leq 2.0$, ($M_J: 1.6 \sim 3.6$); and $\mathcal{M}/\mathcal{M}_{\odot} < 1.0$, ($M_J: 3.6 \sim 4.9$). It is shown that the brighter more massive stars accumulate much more quickly than the fainter less massive stars.

It is noted that unresolved binaries and low mass stars are problems for this technique. Van Albada & Blaauw (1967) assumed that 60% of early type stars are double systems, while Jaschek & Gomez (1970) claimed that approximately 50% of the main sequence stars might be hidden (cf. Bernard & Sanders 1977). According to these assumptions, the total mass of the cluster Pismis 3 can be as large as $\sim 800 \mathcal{M}_{\odot}$.

7 MASS SEGREGATION AND DYNAMICAL STATE

For a dynamically relaxed cluster, the higher mass stars are expected to be settled toward the cluster center, while the fainter, lower mass stars, in the outer regions (Mathieu 1984). The existence of mass segregation is due to the dynamical evolution or is an imprint of the star formation process, or both. At the time of formation, the cluster may have a uniform spatial stellar mass distribution, and because of the dynamical relaxation, the low mass stars may possess larger random velocities, so tending to occupy a larger volume (cf. Mathieu & Latham 1986; McNamara & Sekiguchi 1986; Mathieu 1985).

To display mass segregation in Pismis 3, star counts were made on the main sequence as a function of mass and the distance from the cluster center. The results are shown in Figure 6. The individual curves from left to right are for mass ranges $\mathcal{M}/\mathcal{M}_\odot > 2.0$, $1.0 \leq \mathcal{M}/\mathcal{M}_\odot \leq 2.0$, and $\mathcal{M}/\mathcal{M}_\odot < 1.0$. It suggests that the brighter high-mass stars are concentrated more towards the cluster center and accumulate much more quickly than are the fainter low-mass stars. On the other hand, we are interested whether or not the cluster has reached dynamical relaxation. Applying the dynamical relaxation equation (cf. Tadross 2005, 2006), it is found to be 8.6 Myr, which implies that the age of the cluster is ~ 260 times its relaxation age. Thus we can conclude that Pismis 3 is dynamically relaxed and the evolution is one of the possible causes of mass segregation.

The results from our analysis of refining and determining the fundamental parameters of Pismis 3 using the 2MASS photometry are summarized, and compared with the previous results (CO94) in Table 1.

Table 1 Comparison between the Present Study and CO94

Parameter	The present work	CO94
Center	$\alpha = 08^{\text{h}}31^{\text{m}}21.8^{\text{s}}$ $\delta = -38^{\circ}38'41.2''$	$08^{\text{h}}29^{\text{m}}6^{\text{s}}$ $-38^{\circ}30'0''$
Age	2.24 Gyr	2.0 Gyr
Metal abundance	0.019	0.008
$E(B - V)$	0.67 mag	1.35 mag
R_v	3.2	3.0
Distance Modulus	12.20 ± 0.10 mag	14.70 mag
Distance	2090 ± 95 pc	1500 pc
Radius	$3.5'$ (2.20 pc)	$3.25'$
Membership	450 stars	--
$E(J - H)$	0.22 mag	--
ρ_o	63 ± 2 stars/arcmin ²	--
Core radius	$0.19' \pm 0.04$ (0.20 pc)	--
Tidal radius	12 pc	--
R_g	$8.7 \sim 8.0$ kpc. (see Sect. 3)	--
Z	18 pc	--
X_\odot	-2.0 kpc	--
Y_\odot	0.44 kpc	--
Luminosity fun.	Estimated	--
IMF slope	$\Gamma = -2.37 \pm 0.25$	--
Total mass	$\approx 560 \mathcal{M}_\odot$ (minimum)	--
Relaxation time	8.6 Myr	--
Mass segregation	Achieved	--

Acknowledgements This paper has made use of the Two Micron All Sky Survey (2MASS), which is a joint project of the University of Massachusetts and the Infrared Processing and Analysis Center California Institute of Technology, funded by the National Aeronautics and Space Administration and the National Science Foundation. Catalogues from CDS/SIMBAD (Strasbourg) and Digitized Sky Survey DSS images managed by the Space Telescope Science Institute have been employed.

References

- Bernard J., Sanders W. L., 1977, *A&A*, 54, 569
Bica E., Bonatto Ch., Dutra C. M., 2003, *A&A*, 405, 991
Bica E., Bonatto Ch., Barbuy B., Ortolani S., 2006, *A&A*, 450, 105
Bonatto Ch., Bica E., 2003, *A&A*, 405, 525
Bonatto Ch., Bica E., Girardi L., 2004, *A&A*, 415, 571
Bonatto Ch., Bica E., Santos J. F., 2005, *A&A*, 433, 917
Carraro G., Ortolani S., 1994, *A&A*, 291, 106 (CO94)
Dutra C., Santiago B., Bica E., 2002, *A&A*, 381, 219
Jaschek C., Gomez A. E., 1970, *PASP*, 82, 809
Jeffries R. D., Thurston M. R., Hambly N. C., 2001, *A&A*, 375, 863
King I., 1962, *AJ*, 67, 471
Lyngå G., 1987, *Catalog of Open Cluster Data*, Centre des Donée astronomiques de Strasbourg
Mathieu R., 1984, *ApJ*, 284, 643
Mathieu R., 1985, In: Goodman J., Hut P. eds., *Dynamics of star clusters*, 113, 427
Mathieu R., Latham D., 1986, *AJ*, 92, 1364
McNamara B., Sekiguchi K., 1986, *ApJ*, 310, 613
Montgomery K. A., Marschall L. A., Janes K. A., 1993, *AJ*, 106, 181
Pismis P., 1959, *Bol. Obs. Tonantzintla Tacubaya*, 18, 39
Reid M. J., 1993, *ARA&A*, 31, 345
Salaris M., Weiss A., Percival S., 2004, *A&A*, 414, 163
Salpeter E., 1955, *ApJ*, 121, 161
Spitzer L., Hart M., 1971, *ApJ*, 164, 399
Tadross A. L., 2004, *Chin. J. Astron. Astrophys. (ChJAA)*, 4, 67
Tadross A. L., 2005, *AN*, 326 (1), 19
Tadross A. L., 2006, *AN*, 327 (7), 714
Trumpler R. J., 1930, *LOB*, 14, 154
Van Albada T., Blaauw A., 1967, *CoORB, Uccle B17*, 44